Evaluate Morphological Effect on MR Relaxivity for Bifunctional Au-Fe_3O_4 Heterostructures

Ya-Han Yang[1], Fang-Hsin Lin[1], Yi-Tzu Lu[1], Ruey-An Doong[1], and Hsu-Hsia Peng[1]
[1]*Department of Biomedical Engineering and Environmental Sciences, National Tsing Hua University, Hsinchu, Taiwan*

Introduction: Au-Fe_3O_4 heterostructures are one of the typical magnetic-based nanocomposites that are usually used in biomedical applications, such as dual functional probes for optical imaging and magnetic resonance imaging [1]. The heterostructures have been designed into various architecture, including core-shell, hetero-oligomer, and core-satellite for using as MRI contrast agents. Previous studies have proved that different composites of magnetic-based nanoparticles (NPs) may reveal diverse characteristics while being used as MRI contrast agents [2,3]. Although Au-Fe_3O_4 heterostructures may exhibit weaker T2-decaying effect than pure Fe_3O_4 NPs because of the shielding effect of Au NPs, it is still worthy to investigate Au-Fe_3O_4 heterostructures for their multifunctional characteristics of diagnostic and therapeutic applications. In these decades several magnetite-based heterostructures have been developed for multi-modal imaging probes. However, the effect of morphology of different composite heterostructures on MRI relaxivity is rarely reported. In this study, pure Fe_3O_4 NPs, 5 nm Au dumbbell-like NPs (mAu DBNPs), 10 nm Au dumbbell-like NPs (LAu DBNPs), and 10 nm Au flower-like NPs (LAu FLNPs) were synthesized to demonstrate the T2-decaying effect among different morphological iron-based heterostructures.

Methods: The Fe_3O_4 NPs and Au-Fe_3O_4 heterostructures were synthesized according to previous work [4]. The heterostructured Au-Fe_3O_4 NPs were prepared by thermal decomposition of iron-oleate complex ($Fe(OL)_3$) in the presence of different sizes of Au NPs, saying 5 nm and 10 nm in this study. Dumbbell-like NPs (DBNPs) and flower-like NPs (FLNPs) were manufactured by adding different concentrations of ($Fe(OL)_3$). It has been reported that once the Fe_3O_4 starts to nucleate on an Au NPs, the free electrons from the Au must compensate for the charge induced by the polarized plane at the interface [5]. Since the 5 nm Au NPs have only limited number of electrons, this compensating effect makes all other facets of the Au NPs electron deficient and leads to be unsuitable for multi-nucleation. Consequently, only the dumbbell-like structure of Au-Fe_3O_4 can be composed. As for 10 nm Au NPs, the larger Au provides large surface areas and multiple monocrystalline domains for Fe_3O_4 to nucleation, resulting in the production of dumbbell-like or flower-like heterostructures, depending on the amounts of adding ($Fe(OL)_3$). The dimension and morphology of Fe_3O_4 and Au-Fe_3O_4 heterostructures were examined by analytical transmission electron microscopy (TEM). The concentrations of Fe and Au atom were quantitatively measured by inductively coupled plasma atomic emission spectrometry (ICP-AES) (Kontron, S-35). All MR acquisitions were performed with multi-echo spin echo pulse sequence in a 7 Tesla animal MRI scanner (ClinScan 70/30 USR, Bruker, Germany) with following parameters: TR = 2000 ms, TE = 5.7 to 182.4 ms with an interval of 5.7 ms, number of echoes = 32, voxel size = 0.156 mm × 0.156 mm × 2.0 mm. Seven trials were performed with five concentrations of iron between 0.07~0.42 mM. Various concentrations of the Au-Fe_3O_4 heterostructures were dispersed in bidistilled water. T2 values and r2 relaxivity were evaluated to comprehend the T2-decaying ability of Au-Fe_3O_4 heterostructures with various morphologies and structures. The signal intensities within manually determined regions of interest (ROI) were analyzed by home-developed program with usage of MATLAB (The Mathworks) software. To verify reproducibility, the same samples were performed twice.

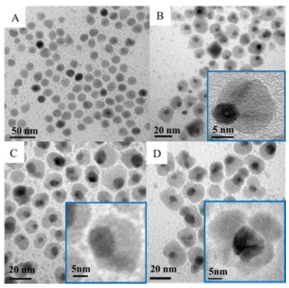

Fig. 1. TEM images of pure Fe_3O_4 (A) and Au-Fe_3O_4 heterostructures of mAu DBNPs (B), LAu DBNPs (C) and LAu FLNPs (D).

Results: Figure 1 showed TEM images of pure Fe_3O_4 (A) and different Au-Fe_3O_4 heterostructures of mAu DBNPs (B), LAu DBNPs (C) and LAu FLNPs (D). The mean diameters of Fe_3O_4, mAu DBNP, LAu DBNP, and LAu FLNP were 13, 13±1, 14±1, and 24±2 nm, respectively. The enlarged insertions demonstrated the appearance of dumbbell-like and flower-like NPs. The T2-decaying effect on Fe_3O_4 heterostructures at various Fe concentrations was shown by T2WI in Fig.2. The signal intensities decreased with increased Fe concentrations. Fe_3O_4 NPs displayed the most strong T2-decaying effect while LAu DBNPs displayed relative weaker T2-decaying ability. Figure 3 displayed the results of R2 (1/T2) of one of the seven trials. A good linearity between R2 and Fe concentrations was observed in each sample, reflected by high correlation coefficients (R^2) of 0.93~1.00. To further compare the T2-decaying ability of each composite, the values of r2 relaxivity, i.e. the slope of fitting curve shown in Fig. 3, were computed. As shown in Fig. 4, the r2 relaxivities were 130.1±16.3, 114.8±20.6, 82.2±31.8 and 104.3±30.8 $mM^{-1}s^{-1}$ for Fe_3O_4, mAu DBNPs, LAu DBNPs, and LAu FLNPs, respectively. The repeated experiment showed the % differences of 1.7%, 4.1%, 6.4%, and 8.2% for Fe_3O_4, mAu DBNPs, LAu DBNPs, and LAu FLNPs, respectively, showing the high reproducibility of measured r2 relaxivities.

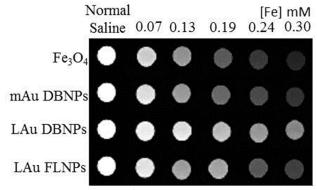

Fig. 2. T2WI of Fe_3O_4 and Au- Fe_3O_4 heterostructures at various Fe concentrations. Fe_3O_4 NPs displayed the most strong T2-decaying effect while LAu DBNPs displayed relative weaker T2-decaying ability.

Discussion and Conclusions: In this study, the T2-decaying ability of various Au-Fe_3O_4 heterostructures with different sizes of Au and with different morphologies of Au-Fe_3O_4 heterostructures was investigated. For 5 nm Au seeds, only dumbbell-like NPs could be produced. In contrast, using 10 nm Au seeds could produce both of dumbbell-like and flower-like NPs. Considering the size of Au, heterostructures with smaller Au NPs have less influence on the magnetic behavior, which attributed to the less contact area and weaker junction effect between smaller Au NPs and Fe_3O_4 NPs [1]. Therefore, mAu DBNPs showed stronger r2 relaxivity than that of LAu DBNPs, which is consistent with a previous report [1]. In addition, the impact of different morphological Au-Fe_3O_4 heterostructures on MRI relaxivity was also investigated in this study. It was found that LAu FLNPs exhibited higher relaxivity than that of LAu DBNPs. This improvement might result from the synergistic effect which more than one iron oxide NPs were linked to one single Au NP, and therefore resulted in magnetic coupling effect among Fe_3O_4 NPs [6]. Accordingly, the magnetic homogeneity surrounding water molecules were deteriorated by multiple tiny magnets around their vicinity. Moreover, the competing forces of inter-particle and intra-particle interactions were shown among FLNPs while DBNPs only have inter-particle interaction. Consequently, the FLNPs revealed stronger T2-decaying effect. In conclusion, using different morphological Au-Fe_3O_4 heterostructures or different sizes of Au NPs as seeds could result in different r2 relaxivity. To manufacture proper configurations of heterostructures are able to enhance T2-decaying effect and can improve image contrast of T2 weighted images in MRI applications.

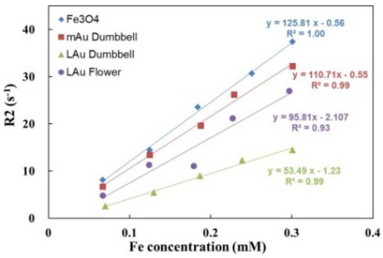

Fig. 3. High linearity was shown between R2 and Fe concentrations, reflected by high R^2 of 0.93~1.00.

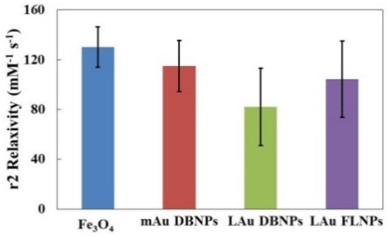

Fig. 4. The r2 relaxivities were 130.1±16.3, 114.8±20.6, 82.2±31.8 and 104.3±30.8 $mM^{-1}s^{-1}$ for Fe_3O_4, and Au-Fe_3O_4 heterostructures.

References: (1) Xu C. et al. Chem. Int. Ed. 2008, 47, 173–176. (2) Zhou, T. et al. J Mater Chem **2012,** 22, 470-477. (3) Garcia, I. et al. Bioconjugate Chem **2011,** 22, 264-273. (4) Lin, F. H. et al. Nano Res **2011,** 4, 1223-1232. (5) Heng Y. et al. Nano Lett., **2005**, 5, 379-382. (6) Berret, J. F. et al. J Am Chem Soc **2006,** 128, 1755-1761.